A Parametric Study of Jet Interactions with Rarefied Flow

C.E. Glass
NASA LaRC, Hampton, VA, USA

1 Introduction

Active control for vehicles traversing the transitional flow regime of an atmosphere is achieved by a reaction control system (RCS), consisting of thrusters strategically placed about the vehicle. When jet plumes from the RCS interact with a local rarefied or transitional flow field, unanticipated aerodynamic forces may result. For example, during the initial bank maneuvers of the first shuttle Orbiter flight, the rolling moment that occurred when the yaw thrusters were fired was less than expected, resulting in greater RCS fuel usage than anticipated. The cause of this discrepancy was attributed to improper scaling of wind tunnel derived RCS interaction correlations to the flight condition [1].

Recently, direct simulation Monte Carlo (DSMC) studies have been performed for the Mars Global Surveyor (MGS) [2] that show the attitude control system (ACS) jets interact with the free stream and cause thrust reversal during the aerobraking maneuver in the transitional regime. That is, a net torque is produced in the direction opposite from that induced by the ACS thruster; the ACS jet plume shadows a downstream portion of the spacecraft from the free stream flow, which causes lower local surface pressure than without the shadowing. Therefore, it is important to understand the interaction of an ACS or RCS jet plume with the surrounding rarefied flow field and surface to accurately incorporate the effects of the interaction in the vehicle design and aerodynamic control laws during a mission.

2 Problem Description

The purpose of this paper is to report results of a numerical study of a continuum jet interaction with a rarefied flow. The free stream number density (n_∞) of a baseline case is varied to produce changes in the interaction strength and provide insight into the underlying fluid mechanics of these interactions. A recently reported numerical technique [3] is used in

Case	1 (baseline)	2	3	4	5
$n_\infty/n_{\infty,baseline}$	10^0	10^{-1}	$10^{-1.5}$	$10^{-1.75}$	10^{-2}
, $=(\rho V^2)_{jet}/(\rho V^2)_\infty$	38.23	382.3	1209	2150	3823

Table 1: Variation of free stream number density and ratio of jet to free stream momentum flux for the cases studied.

this study. The technique uncouples computational fluid dynamics (CFD) applied to the jet flow field and DSMC solutions for the interacting and rarefied flow field at an appropriate breakdown surface [4] to produce a flow solution for the entire flow field from the two different numerical methods.

The baseline case modeled by the present numerical study corresponds to a jet interaction experiment performed by Keith Warburton at the Defence Evaluation and Research Agency (DERA) low density wind tunnel. A schematic diagram of the experimental flat plate model is shown in Fig. 1. Free stream nitrogen flow about the sharp leading edged flat plate had a nominal Mach number of 9.84, static temperature of 65K, and static pressure of 5.4 Pa, resulting in a Reynolds number based on the plate length of 0.15 m, Re_L, equal to 15,900. For the present study, the jet gas was argon and the nozzle plenum conditions were T = 300K and p = 34.5 kPa, addressing one of cases examined by Warburton.

It was shown in Ref. [3] that this test condition provides a rarefied flat plate flow for the baseline 3-D jet interaction numerical study. In addition to the baseline case (case 1), four other 3-D jet interaction cases were examined in the present study (See Table 1.) to establish parametric variation. The baseline free stream density is lowered by 1, 1-1/2, 1-3/4, and 2 orders of magnitude, which are cases 2, 3, 4, and 5, respectively, while holding all other free stream conditions constant. By varying the free stream density, the effect of the jet interaction on the flow field and on the flat plate surface is systematically examined.

3 Numerical Technique

Details of producing an uncoupled CFD-DSMC solution are given in Ref. [3], and a general overview of the procedure is given below. For the present study, CFD solutions were obtained using the General Aerodynamic Simulation Program ($\mathcal{GASP}$) [5], a commercially available finite volume Navier-Stokes flow solver from AeroSoft, Inc. DSMC solutions were obtained by the DSMC analysis code (DAC) of LeBeau at NASA JSC. (For example, see Refs. [3], [6], and [7].) The uncoupled solution methodology requires a boundary between the undisturbed continuum jet flow and the interacting portions of the free stream and jet flow be defined. This is accomplished

using a value of the Bird breakdown parameter [4], P, which assures that the CFD portion of the flow solution is not influenced by the jet interaction region, that is, it remains symmetric as is discussed and shown below.

To determine the boundary between the CFD and DSMC flow domains, CFD solutions of the entire interacting flow field, from the jet plenum to the free stream, were obtained and analyzed. These solutions contain the continuum portion of the jet flow as it expanded from the nozzle exit, which allows an analysis by the breakdown parameter. Twelve jet interaction cases were computed with the CFD: fixed nitrogen free stream properties with jet gases of helium, nitrogen, argon, and carbon dioxide at plenum pressures of 17.4, 34.5, and 51.7 kPa. A typical centerline number density contour from a CFD solution is shown in Fig. 2, which is an interacting argon jet at a plenum pressure of 34.5 kPa modeled in the present study as the baseline case. Note that number density contours are normalized by Loschmidt's number, n_o, the standard number density of air at T = 273K and p = 101.325 kPa [4].

An analysis of the CFD solutions was performed using the Bird breakdown parameter to determine an appropriate breakdown surface of the jet plume where no interaction effects were present at the breakdown surface. A sample of these results is shown in Fig. 3. Note that the breakdown surface for $P = 0.01$ on the left side of Fig. 3 shows a smooth, regular surface of a volume of revolution; however, the breakdown surface on the right side of the figure ($P = 0.02$) has an irregular diagonal cut on the upper windward portion. The irregular cut on the breakdown surface occurs at the location of the compression region between the jet and the free stream. Based on this analysis, a breakdown surface influenced by the free stream to jet interaction will exhibit the irregular surface feature. Therefore, a boundary can be established where the interaction does not influence the flow at or inside the surface. Results of analyzing the twelve CFD solutions to determine the largest value of breakdown parameter where the breakdown surface is smooth and not affected by the interaction are shown in Fig. 4. The breakdown parameter values shown in Fig. 4 are correlated with a nondimensional parameter G_{jet}/G_{∞}, with G defined by Eq. 1 as:

$$G = \frac{nV}{\nu/(\lambda d)} \tag{1}$$

which is the ratio of the number density flux, nV, and the molecular collision probability flux, $\nu/(\lambda d)$.

Given the curve fit relationship shown in Fig. 4, the two different solution domains (CFD and DSMC) can be uncoupled, which has been performed for the five cases presented in the following section. The jet nozzle and plume are calculated using CFD. Typical grid and flow field results of the CFD calculations are shown in Fig. 5. An appropriate breakdown parameter

value is obtained from the curve in Fig. 4, which defines the jet inflow location for the DSMC. A breakdown parameter value of $P = 0.01$ was chosen for the baseline (case 1), and $P = 0.02$ was chosen for the other cases. $P = 0.02$ represents the upper limit of the continuum regime for an expanding flow [4]. Next, the free stream and interacting regions of the flow, excluding the continuum noninteracting portion of the jet plume, are predicted using DAC. The DAC requires the surface, which the flow is being modeled about, be triangulated. A triangulated representation of the flat plate model for the present study is shown in Fig. 6. Note the close view of the jet breakdown surface shown on the upper right side of the figure.

4 Results and Discussion

Number density contours and flow streamlines at the plane of symmetry for the five cases described above are presented in Figs. 7 to 11. A comparison of these figures shows that as the free stream number density decreases, the extent of the jet interaction bow shock increases. Also, comparing Figs. 7 and 8, the forward separation vortices become larger for decreasing free stream number density, and as shown in Fig. 11, when the free stream number density is decreased by two orders of magnitude below the baseline case, the forward separation vortices are not present. This is significant because the forward separation vortices allow the flat plate shock layer flow and jet plume flow to stagnate along a reattachment line. Without the separation region present, the jet gas is directed outward away from the nozzle with no surface stagnation. The boundary where the free stream number density just supports the formation of the forward separation region is between cases 3 and 4, that is, when the value of jet to free stream momentum flux, , $\gtrsim 2000$. (See Table 1.)

The normalized surface pressure along the model centerline is presented next in Fig. 12. Note that pressure is normalized by the free stream momentum flux for each case. The figure shows that as the free stream number density decreases, the forward extent of the jet interaction influence increases and broadens over the flat plate surface. For case 5, which has the lowest free stream number density, the jet interaction influence has moved upstream and is felt at the flat plate leading edge. (See Figs. 11 and 12.)

Normalized shear stress, $\tau_x/(\rho V^2)$, along the flat plate centerline is presented in Fig. 13 for all five cases. The sign of the shear stress indicates the local flow direction just above the flat plate surface; that is, a positive value indicates the free stream flow direction, and a negative value indicates reversed flow, opposite the free stream direction. Immediately upstream of the jet nozzle exit (x = 0.125 m), flow just above the plate surface is in the reverse direction as indicated by the negative shear stress. Further upstream, the local shear stress becomes positive for all cases. For cases 1, 2,

and 3, local shear stress changes sign again, indicating a separated, reversed flow region; the separation region just upstream of the nozzle exit is also shown by streamlines in Figs. 7, 8, and 9, respectively. However, unlike cases 1, 2, and 3, the surface shear stress is everywhere positive forward of the initial reversed flow region for cases 4 and 5, as shown in Fig. 13, indicating no separated flow near the surface. Also, the flow streamlines for case 4 (See Fig. 10.) do show a vortical structure above the plate surface forward of the nozzle exit, but not near the surface. For the lowest free stream density condition (case 5 shown in Fig. 11), no vortical structure is evident, probably because the free stream flow is not sheared by the jet flow sufficiently to cause a vortex.

To assess the integrated effect of the jet interaction on the upper surface of the flat plate, the moment coefficient, $C_{m,y} = 2M_y/(\rho V^2 AL)$, which is about the y-axis at the center pivot of the upper plate surface (x = 0.075 m), as a function of jet to free stream momentum flux ratio, , , is presented as Fig. 14. Note that moment contributions on plate surfaces other than the upper surface are neglected to isolate jet interaction effects on the upper surface only. At higher momentum flux ratio (cases 1, 2, and 3), the moment coefficient is positive and increases with decreasing momentum flux ratio because the magnitude and extent of normalized surface pressure increases over the aft portion of the plate surface as shown in Fig. 12. However, between cases 3 and 4, there is a downward turn of the moment coefficient curve, and at the momentum flux ratio of case 5, the moment coefficient is negative. The jet interaction effect has fed forward and causes a nose down or negative pitch for case 5. High pressure on the forward portion of the plate is also shown in Fig. 12 for case 5. In addition, the number density contours in Fig. 11 show that the jet interaction influences the flow field to the leading edge of the flat plate.

5 Concluding Remarks

Three-dimensional computational techniques, in particular the uncoupled CFD-DSMC of the present study, are available to be applied to problems such as jet interactions with variable density regions ranging from a continuum jet to a rarefied free stream. When the value of the jet to free stream momentum flux ratio, , $\gtrsim$ 2000 for a sharp leading edge flat plate, no forward separation vortices induced by the jet interaction are present near the surface. Also, as the free stream number density, n_∞, decreases, the extent and magnitude of normalized pressure increases and moves upstream of the nozzle exit. Thus, for the flat plate model, the effect of decreasing n_∞ is to change the sign of the moment caused by the jet interaction on the flat plate surface.

References

[1] Scallion, W.I., Compton, H.R., Suit, W.T., Powell, R.W., Blackstock, T.A., and Bates, B.L., "Space Shuttle Third Flight (STS-3) Entry RCS Analysis," AIAA 83-0116.

[2] Shane, R.W., Rault, D.F.G., and Tolson, R.H., "Mars Global Surveyor Aerodynamics for Maneuvers in Martian Atmosphere," AIAA 97-2509.

[3] Glass, C.E. and LeBeau, G.J., "Numerical Study of a Continuum Sonic Jet Interacting with a Rarefied Flow," AIAA 97-2536.

[4] Bird, G.A., *Molecular Gas Dynamics and the Direct Simulation of Gas Flows*, Clarendon Press, Oxford, 1994.

[5] AeroSoft, *GASP Version 3, The General Aerodynamic Simulation Program, Computational Flow Analysis Software for the Scientist and Engineer, User's Manual*, AeroSoft, Inc., Blacksburg, Virginia, 1996.

[6] Wilmoth, R.G., Le Beau, G.J., and Carlson, A.B., "DSMC Grid Methodologies For Computing Low-Density, Hypersonic Flows About Reusable Launch Vehicles," AIAA 96-1812.

[7] LeBeau, G.J., "A Parallel Implementation of the Direct Simulation Monte Carlo Method," to be published in *Computer Methods in Applied Mechanics and Engineering*, 1998.

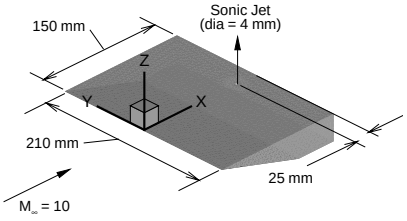

Figure 1: Flat plate model.

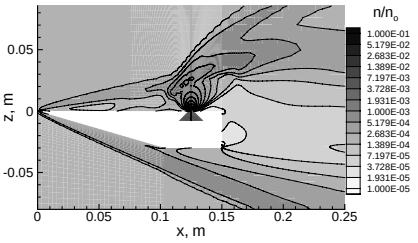

Figure 2: Number density contours from CFD solution of baseline case.

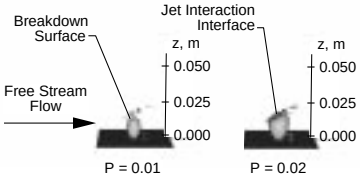

Figure 3: Jet breakdown surface from CFD solution.

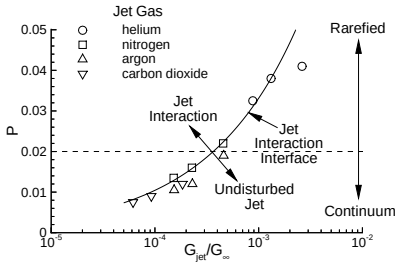

Figure 4: Correlation of breakdown parameter with jet interaction strength.

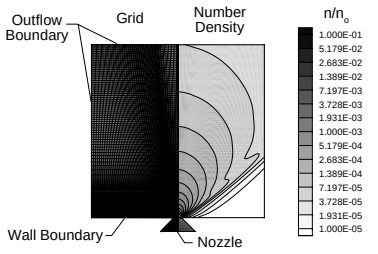

Figure 5: CFD grid and number density contours of axi-symmetric free expanding jet.

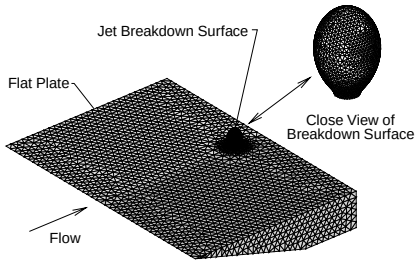

Figure 6: Triangulated flat plate and jet breakdown surface.

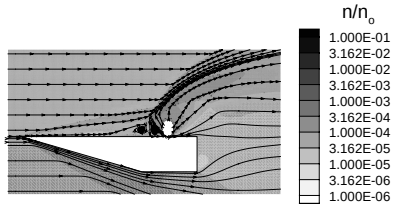

Figure 7: Number density contours and streamlines for case 1 (baseline, , = 38.23).

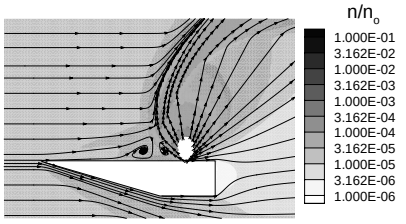

Figure 8: Number density contours and streamlines for case 2 (, = 382.3).

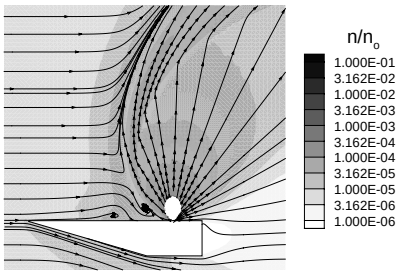

Figure 9: Number density contours and streamlines for case 3 (, = 1209).

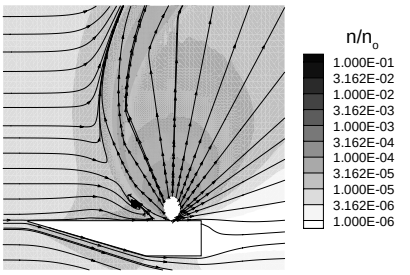

Figure 10: Number density contours and streamlines for case 4 (, = 2150).

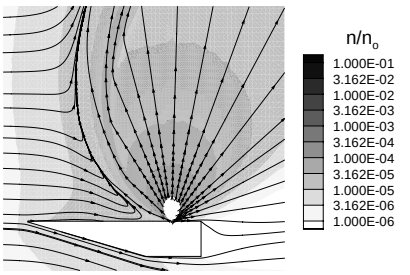

Figure 11: Number density contours and streamlines for case 5 (, = 3823).

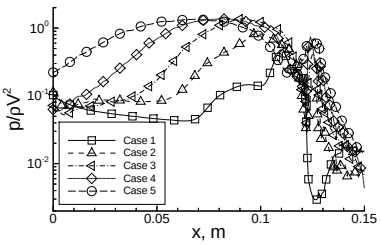

Figure 12: Normalized pressure on flat plate centerline.

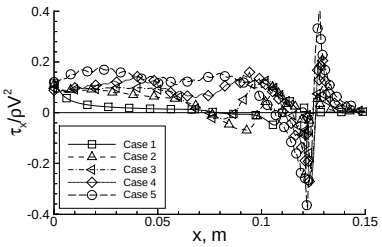

Figure 13: Normalized shear stress on flat plate centerline.

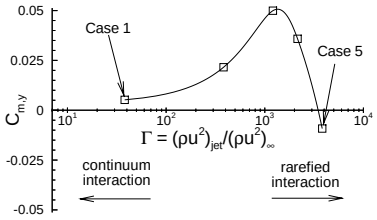

Figure 14: Moment coefficient as a function of the jet to free stream momentum flux ratio.